LA-UR- 10-04680

Approved for public release; distribution is unlimited.

Title: Active Interrogation Using Energetic Protons

Author(s): C. L. Morris, Kiwhan Chung, Steven Greene, Gary Hogan, Mark Makela, Fesseha Mariam, Edward C. Milner, Matthew Murray, Alexander Saunders, Randy Spaulding, Zhehui Wang, Laurie Waters, Frederick Wysocki, Los Alamos National Laboratory, Los Alamos, NM 87544

Intended for: Institute of Nuclear Materials Management
51th Annual Meeting
July 11-15, 2010
Marriott Baltimore Waterfront Hotel
Baltimore, Maryland

Los Alamos
NATIONAL LABORATORY
EST. 1943

Los Alamos National Laboratory, an affirmative action/equal opportunity employer, is operated by the Los Alamos National Security, LLC for the National Nuclear Security Administration of the U.S. Department of Energy under contract DE-AC52-06NA25396. By acceptance of this article, the publisher recognizes that the U.S. Government retains a nonexclusive, royalty-free license to publish or reproduce the published form of this contribution, or to allow others to do so, for U.S. Government purposes. Los Alamos National Laboratory requests that the publisher identify this article as work performed under the auspices of the U.S. Department of Energy. Los Alamos National Laboratory strongly supports academic freedom and a researcher's right to publish; as an institution, however, the Laboratory does not endorse the viewpoint of a publication or guarantee its technical correctness.

Form 836 (7/06)

Active Interrogation Using Energetic Protons

C. L. Morris, Kiwhan Chung, Steven Greene, Gary Hogan, Mark Makela, Fesseha Mariam, Matthew Murray, Alexander Saunders, Randy Spaulding, Zhehui Wang, Laurie Waters Frederick Wysocki Los Alamos National Laboratory, Los Alamos, NM 87544

Energetic proton beams provide an attractive alternative when compared to electromagnetic and neutron beams for active interrogation of nuclear threats because they have large fission cross sections, long mean free paths and high penetration, and they can be manipulated with magnetic optics. We have measured time-dependent cross sections and neutron yields for delayed neutrons and gamma rays using 800 MeV and 4 GeV proton beams with a set of bare and shielded targets. The results show significant signals from both unshielded and shielded nuclear materials. Measurements of neutron energies yield suggest a signature unique to fissile material. Results are presented in this paper.

Introduction

Active interrogation with sources of gamma rays and neutrons is being explored as a possible method for the inspection of various cargos for nuclear materials or devices.[1] We discuss an alternative—proton interrogation, which fundamental principles suggest would provide a much better source.

Active interrogation has been shown to increase the radiation signature of unshielded or lightly shielded nuclear material enormously. The delayed neutron and gamma signatures can uniquely establish the presence of fissionable and fissile material. The difficulty is that even this increased signal can be significantly reduced by heavily shielding the target.

As an example, the load limit of a standard shipping container of about 20 metric tons allows shielding configurations that are very difficult to penetrate with conventional nuclear probes. Consider a shielded volume of 50 cm in radius and 100 cm long in the center of a $2.5\times2.5\times10$ m^3 container. Such a volume could be shielded with 10 cm of lead and 90 cm of polyethylene on all sides. The lead would provide gamma ray shielding, and the polyethylene, neutron shielding. An inner layer of borated polyethylene would absorb thermal neutrons, and the outer polyethylene would absorb a large fraction of the 0.4 MeV gamma rays emitted in the neutron capture. A schematic view of what such a shield might look like is shown in Figure 1.

The weight of such a shield configured as hemispherical end caps on a 50-cm-long cylinder is calculated to be about 10 tons. When one considers that even the polyethylene shield (180 g/cm^2) cannot be penetrated without very large x-ray doses.

Intermediate energy protons (~1 Gev) have much longer attenuation lengths than the more conventional probes, and can penetrate thick cargoes. In addition they have large cross sections[2], 1.0 barn, for producing fission in actinide materials. Because of the obvious benefit of the high penetration of protons and much lower doses needed to produce a signal we have undertaken a program to study the use of protons for stand-off active interrogation.

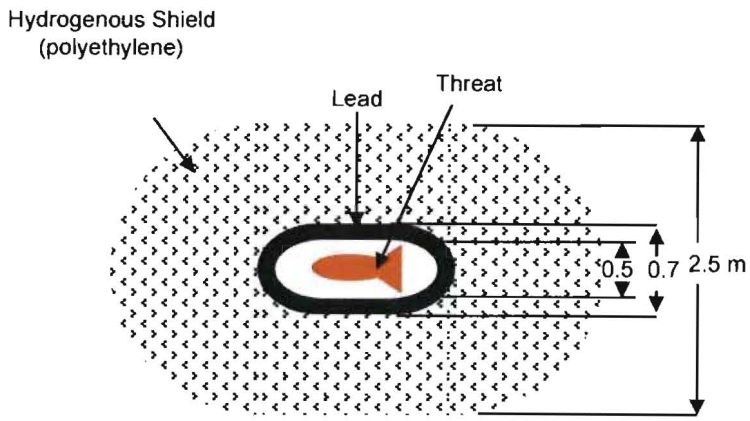

Figure 1. Schematic picture of a heavily shielded target.

Cross section and yield studies

We have measured the delayed neutron production cross sections on a range of targets spanning the periodic table of the elements. Sample sizes were in the range of 10–100 g.

The targets were irradiated with short single pulses of up to 10^{11} 800-MeV protons provided by the LANSCE accelerator at Los Alamos National Laboratory (LANL). The experiment used the beam-on-demand format that has been implemented for proton radiography. The beam transmitted through the target was imaged onto a scintillator and camera system for a direct measurement of the number of protons passing through the target volume.

The number of delayed neutrons, dC, collected in the detector in time $d\tau$ is given by:

$$dC = \frac{d\sigma_{DN}}{dt} \cdot \mathrm{P} \cdot N \cdot \varepsilon \, d\tau \qquad (1)$$

where $\frac{d\sigma_{DN}}{dt}$ is the delayed-neutron production cross section; P is the number of protons incident upon the target; N is the atomic thickness of the target in nuclei/mb; and ε is the total efficiency of the detector. We have assumed that sufficient time has passed that the prompt neutron signal from room scattering has decayed to zero and we have neglected any secondary activation through various (n, x) reactions. The cross section is then directly given by inverting the above equation:

$$\frac{d\sigma_{DN}}{dt} = \frac{dC}{d\tau} \frac{1}{\mathrm{P} \cdot N \cdot \varepsilon} \qquad (2)$$

The incident number of protons, P, is given by P = kp, where p is the total number of protons summed over all beam pulses and k is a parameter describing the ratio of protons that passed entirely through the target. We measured $k = 0.8$ for the uranium targets and $k = 1$ for all other targets by imaging the transmitted proton beam on a phosphor/camera system.

The atomic thickness is given by $N = \frac{\rho_l \cdot \lambda \cdot N_A}{M} \cdot 10^{-27}$, where λ is the mass thickness of the target, M is the molecular mass, N_A is Avogadro's number, 10^{-27} converts from cm^2 to mb, and ρ_l is the density of the target. For the ^{18}O water targets, we have scaled the density of normal water by the ratio of molecular atomic masses, 20/18.

The total delayed neutron efficiency was measured with a ^{252}Cf standard. For all of our analysis we have taken the efficiency to be energy independent. The actual neutron efficiency is neutron energy dependent. We estimate that this typically introduces a factor of ~30% uncertainty in the absolute cross-section measurements.

An empty-target run was subtracted from each target in run. The background from the environment was assumed to be constant and the target-specific background was assumed to be negligible.

Neutron cross section results

800-MeV Protons

We used the 800-MeV proton beams from the LANSCE accelerator to measure the delayed neutron cross sections on the thin targets. The time-integrated total cross sections as a function of atomic mass are summarized in Figure 2. Oxygen-18 has the largest delayed neutron cross section other than ^{235}U and ^{238}U.

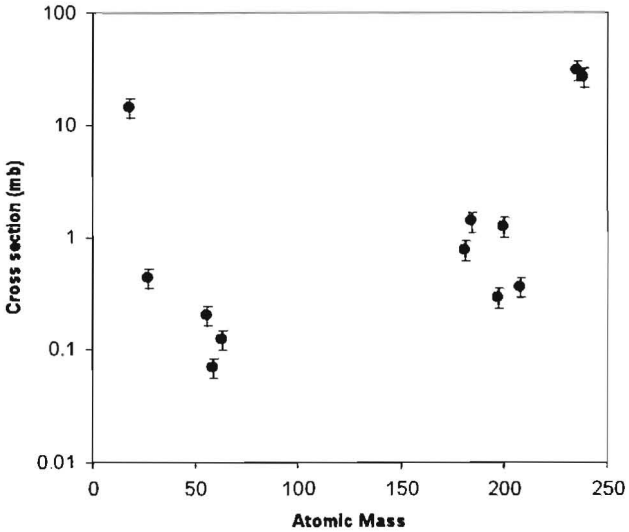

Figure 2. Time-integrated delayed neutron production cross sections as a function of atomic mass for 800-MeV protons.

The time-dependent neutron cross sections, Figure 3, have shown that, although the time-integrated delayed neutron cross sections are comparable among ^{18}O, ^{235}U, their neutron time-decay characteristics are quite different. Specifically, for t > 2 seconds, ^{18}O has a delayed-neutron decay time of approximately 4 sec (from the 4.17-second half-life of ^{17}N to be exact, as will be discussed below), but ^{235}U, ^{238}U decays have to be characterized by multiple decay curves. Furthermore, all other targets have delayed-neutron decay curves similar to ^{18}O. Therefore, we conclude that except for ^{235}U and ^{238}U, delayed neutron productions by all other material are principally from a family of precursors having half-lives in the range of 3–6 seconds. One precursor in this group, ^{17}N, having a half-life of 4.17 seconds, dominates the decay. Others, in the 3–6 second time range, are also produced, but with much lower cross sections. We have ignored the short (< 1 sec) time-decay characteristics here, because the neutron fluxes could not be measured accurately because of instrumental dead time.

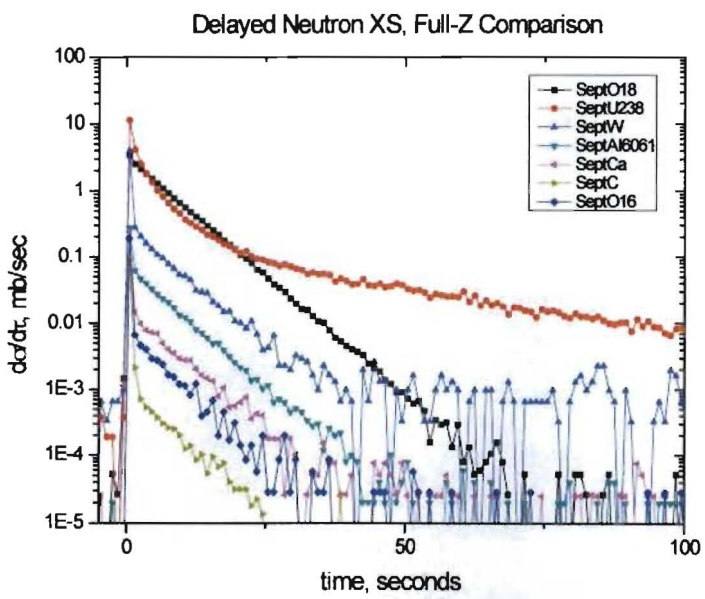

Figure 3. Delayed neutron production as a function of time for various simple targets. All targets show a characteristic delay time of ~4 sec. except for ^{238}U.

The 4-second decay time of neutron emissions are primarily from ^{17}N, which has a characteristic beta-delayed neutron emission time of 4.17 sec.[3, 4] In the case of ^{18}O in a proton beam, ^{17}N is produced by the quasi-free knockout process $^{18}O(p,2p)^{17}N$.

Production of ^{17}N, together with ^{9}Li and ^{16}C, by 1.0 GeV and 2.8 GeV proton beams striking materials other than ^{18}O, have been measured experimentally and the experimental data were compared with calculations.[5] Production of ^{17}N from light nuclei is through knockout, that is, (p,xp) reactions, and from heavier targets through evaporation from excited knock-out cascade daughter products. By comparing the half-lives of ^{9}Li, ^{16}C, and ^{17}N in Table 5, it is clear that ^{17}N is the predominant low-Z contributor to delayed neutron productions for time longer than a few seconds.

Nuclide	Half-life (sec)	Total neutron branch (%)
^{9}Li	0.176 ± 0.001	75 ±15
^{16}C	0.74 ± 0.03	
^{17}N	4.16 ± 0.01	95 ±1

Table 1. Comparison of a few longest half-life low-Z delayed-neutron precursors.

Dostrovsky measured ^{17}N production cross section for energetic proton beams on uranium to be 1.1 mb for 1 GeV and 6.3 mb for 2.8 GeV. Both of these cross sections are larger than their corresponding delayed fission neutron cross sections, as shown in Table 2. This table, from Dostrovsky's 1965 paper, describes the extracted delayed-neutron contributions from the fission fragment groups usually used in characterizing delayed neutrons from fissionable materials.

TABLE IV. Cross sections for the production of fission-product delayed-neutron-emitting groups from uranium with 1- and 2.8-GeV protons.

Half-life group (sec)	Cross section (mb) 1 GeV	Cross section (mb) 2.8 GeV	Fractional yield 1 GeV	Fractional yield 2.8 GeV	U^{235} [a]	U^{238} [a]
55	0.17±0.02	0.20±0.02	0.038±0.007	0.046±0.006	0.038	0.013
22	0.62±0.10	0.60±0.06	0.14 ±0.02	0.14 ±0.02	0.21	0.14
6	0.8 ±0.3	1.1 ±0.5	0.18 ±0.07	0.27 ±0.09	0.19	0.16
2.2	1.8 ±0.2	1.4 ±0.6	0.41 ±0.07	0.33 ±0.13	0.41	0.39
0.5	1.1 ±0.2	1.0 ±0.4	0.23 ±0.05	0.22 ±0.08	0.13	0.22
0.18					0.026	0.075
Total	4.5 ±0.4	4.3 ±0.9				

[a] Fission spectrum neutron fission. See Ref. 19.

Table 2. Cross sections and fraction yields for the production of fission-product delayed-neutron-emitting groups from uranium with 1- and 2.8-Gev protons.
Table from Dostrovsky et al. (1965). Columns 6 and 7 are the yields measured by Keepin et al. (1957).

The precursor of the delayed neutron emission for the 55-sec group has been identified to be ^{87}Br, which has a half-life of 55.6 sec before beta-decaying into two excited states of ^{87}Kr, the higher energy state of which emits a neutron to turn into ^{86}Kr, the stable nuclide. The principal precursors of the 22-sec delayed neutron group are ^{137}I, which has a 24.5-second half-life and ^{88}Br, which has a 16.3-second half-life.

Analysis of the neutron signals at early times (< 1 sec) has found an enhanced neutron production rate compared to Keepin's multigroup fit. This may arise from the many varieties of short-lived beta-delayed precursors that spallation and fragmentation reactions can produce, but cannot be produced by fission. Room return and background produced by scattered protons interacting with the structures around the targets (the target ladder and concrete floor and walls, for example) also contribute to this effect. The presence of the latter two effects greatly complicates analysis of delayed neutrons at msec times. The bulk of this focuses on long-time behavior (t > 2 s) where the differences between actinide targets and lighter elements is the largest. Figure 4 displays the data of Figure 3 on an exponential time axis to show the short time behavior.

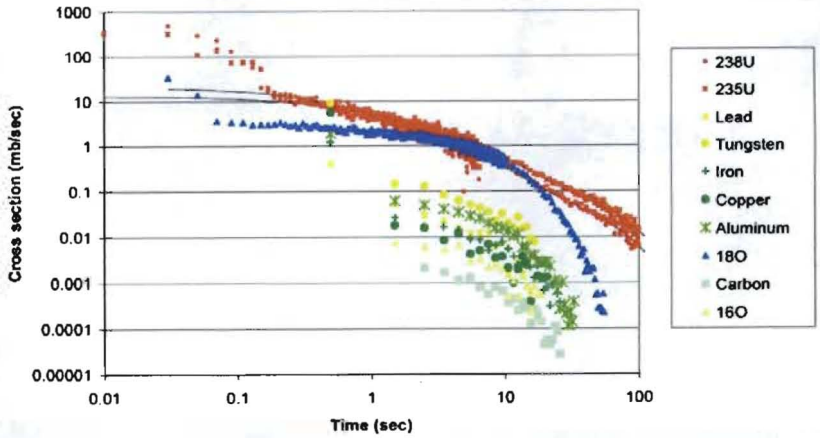

Figure 4. Observation of enhanced delayed neutron production in early times with respect to the proton pulse.

4 GeV Protons

Delayed neutron cross-section data, shown in Figure 5, were obtained using the Alternating Gradient Accelerator (AGS) at Brookhaven National Laboratory. The data were taken with a setup very similar to that used for obtaining the 800 MeV data. The delayed-neutron arrival time spectra verify the major conclusions of our previous measurements. The longer time-delayed neutron signals are much larger from the uranium targets than from normal materials. In this experiment it appears that a small but significant fraction of the signals from the other targets was induced in the room from scattered particles. This is the only way to understand the apparent ^{17}N delayed neutrons (distinctive because of the 4.17-sec lifetime) produced with the graphite target.

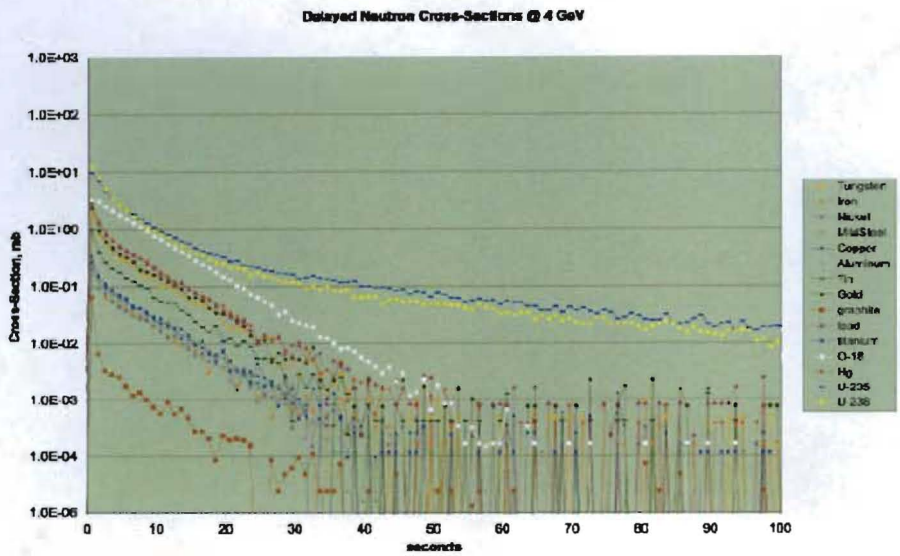

Figure 5. Delayed neutron cross section as a function of time for thin targets and 4-GeV protons.

We compared the cross sections between the 800-MeV and 4-GeV beams. For ^{235}U, while the longer time behavior (decay constant) seems to be the same, the shorter time behavior (< 30 sec) is seen to be somewhat different. Several factors contribute to this, most notably an enhanced ^{17}N component in the 4-GeV data. They include different room background at LANL and BNL, and as in Dostrovsky's work, the different dependence on proton energy for different delayed-neutron groups. This issue is being addressed more quantitatively. The trend of the ^{238}U is similar to ^{235}U (see Figure 7), when the proton energy changes. However, the details might be different. In contrast, for a simpler target, such as oxygen-18, the decay-time constants are essentially the same for the two energies, except that the higher energies produce more neutrons, consistent with the previous work.

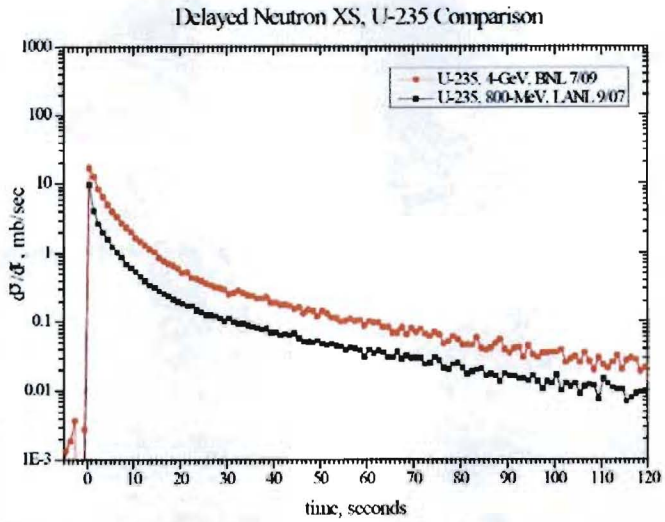

Figure 6. Comparison of the time-dependent delayed-neutron production cross section for the 800-MeV and 4-GeV beams, with a ^{235}U target.

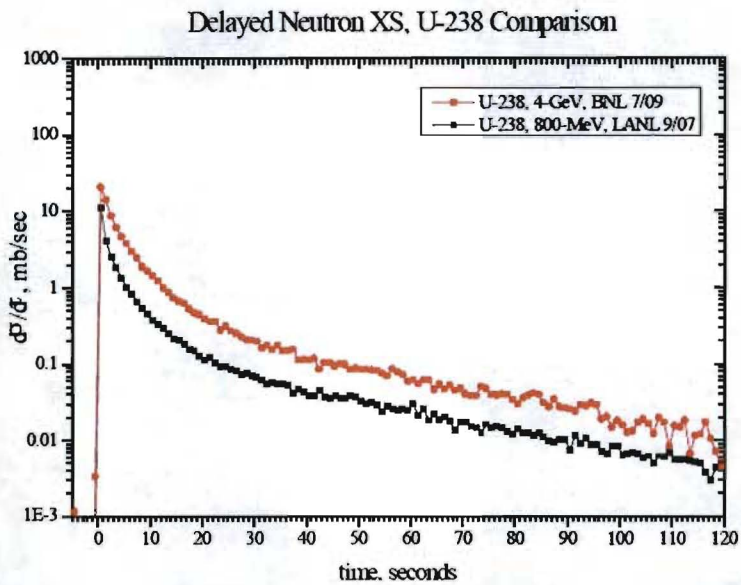

Figure 7. Comparison of the time-dependent delayed-neutron production cross section for the 800-MeV and 4-GeV beams, with a ^{238}U target.

Standoff measurement of delayed neutrons

We took data with an array of 72 moderated ^{3}He tubes, with a standoff distance ranging from 10–30 m at LANL, and up to 100 m at BNL. The background at 100 m was large at BNL so we moved the detector to the 50-m location later.

Experimental Setup

Figure 8 shows a DU target inside a 3-in.-thick borated poly box in Line-C (LANL) for the 800-MeV experiment. The proton beam position was calibrated using a small fluorescent screen monitor. We also set up a 250-gallon water tank filled with tap water. The detector was positioned at different distances along a straight line, which was approximately perpendicular to the proton beam. The measurement showed, however, that the water does not make any noticeable difference to the neutron signal.

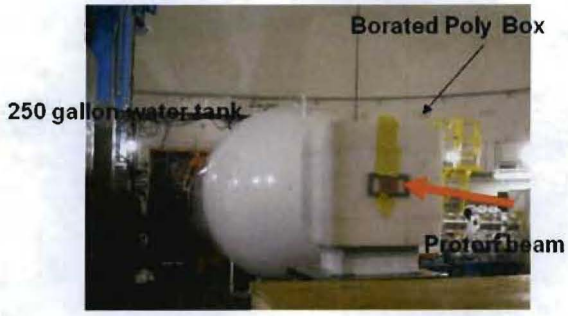

Figure 8. Setup of the 19-kg DU target inside the borated HDPE box with a 250-gallon water tank as the background.

LANL 800-MeV Protons

The delayed neutrons as a function of time for DU, DU + Pb, DU + Pb + 3 in. of borated poly, etc., are shown in Figure 9. The observations are qualitatively the same as when the smaller ^{3}He detector is placed at ~1 m away from the target: (a) neutron emissions with a characteristic time longer than ~4 sec only come from targets with a DU core in place; (b) Pb shielding around the DU increases the number of neutrons; (c) HDPE shielding reduces the delayed neutron signals, with the reduction proportional to the shielding thickness; (d) borated poly can attenuate the neutron fluxes even more than HDPE of the same thickness. The time integrated signals for the different geometries are compared in Figure 10. The signal to noise is large even for the most shielded configurations.

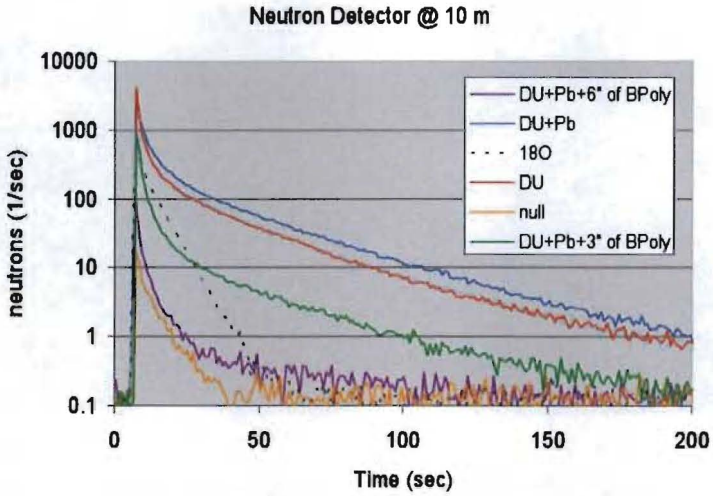

Figure 9. Neutron flux as a function of time for different shielding configurations around a 4"×4"×4" DU cube. Oxygen-18 included to display the 4.17-sec lifetime curve.

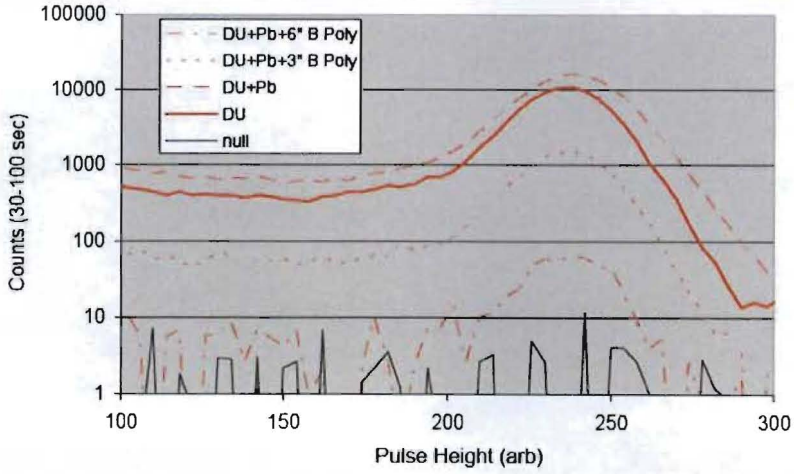

Figure 10. Time-integrated (between 30–100 sec after the proton pulse) neutron signals from the neutron detector at 10-m standoff distance from the production target. Signals are significantly above the background, even with a heavy shielding of 6-in.-thick borated poly.

Using the measured delayed neutrons, the detector efficiency and solid angle, and assuming that each fission produces 0.5% delayed neutron, one can estimate the number of fission produced per proton. The fissions per proton are compared with this approximate model in Table 3.

	Fissions/p
Measured	2.33
model	1.6

Table 3. Comparison of the measured fissions per proton with an MCNPX model.

BNL 4-GeV Protons

The results for 50 m are summarized in Figure 11. The 4-second signals are much more pronounced than at LANL. Only signals from bare DU and DU + Pb are distinguishable from the background. The beam tunnel both reflects and guides neutrons and produces neutrons because of spallation interactions produced by proton beam halo. Some of these interactions are much closer to the detector than the target. The beam stop, which is located ~15 m past the target is also a source of background. Further investigations of the background issues are underway.

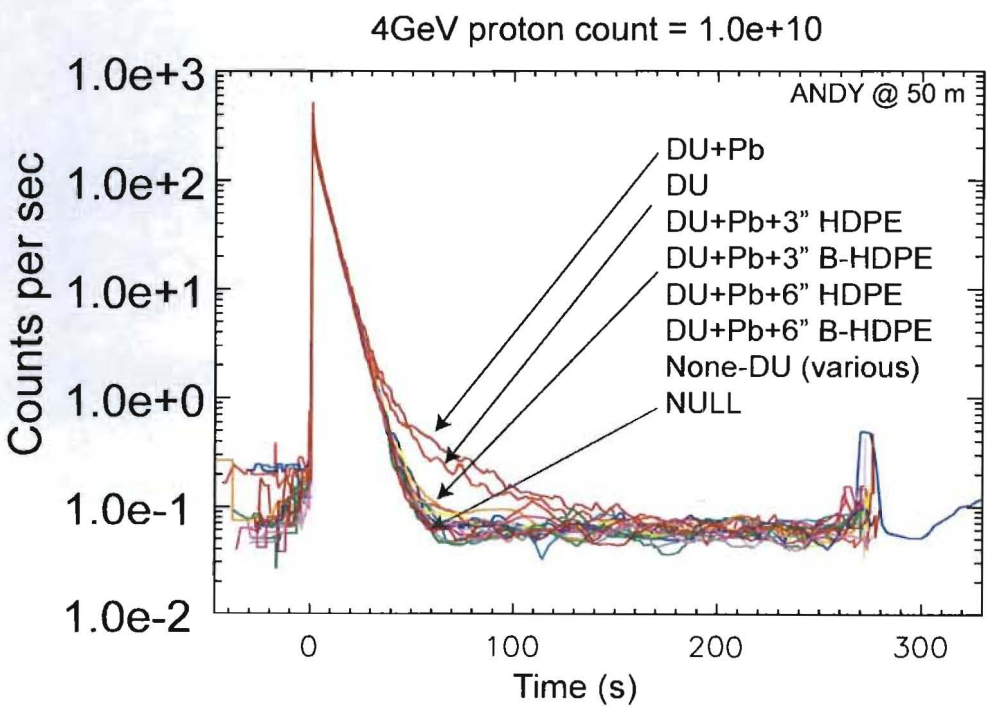

Figure 11. Delay neutrons detected at 50 m away by the neutron detector for various threat objects hit by the 4-GeV beam. The 4-sec signals are much more pronounced than at LANL.

Delayed-neutron induced fission

Although the neutron measurements from moderated detectors, such as ^{3}He, show very similar decay features for ^{238}U and ^{235}U, we have recognized that ^{238}U can be distinguished from ^{235}U by measuring the delayed neutron energy spectrum.

There is a sharp increase in the fission cross sections in ^{238}U for neutron energies around 1.3 MeV, below which ^{238}U fission is very small. This is quite different from ^{235}U and ^{239}Pu, in which both thermal neutrons and MeV fast neutrons can induce fissions (see Figure 12). Delayed neutrons, which typically have a mean energy from

0.25 to 0.4 MeV, can induce prompt fissions in ^{235}U but not in ^{238}U. Therefore, neutron energy measurements as a function of time (relative to the proton pulse) with a threshold > 1 MeV would allow distinguishing ^{238}U and ^{235}U targets. An energy threshold $E_n > 1.7$ MeV would remove ^{17}N background, and enable signatures using delayed neutrons at earlier times.

Conclusions

Cross sections from delayed neutron emission show significant differences between actinide targets and other materials. We have shown that these differences can be used to find signatures of fissionable materials. Experiments at both 800 and 4000 MeV have demonstrated standoff active interrogation with energetic proton beams. Work is proceeding to study delayed neutron induced prompt fissions on enriched targets. This technique shows distinctive signatures of fissile material.

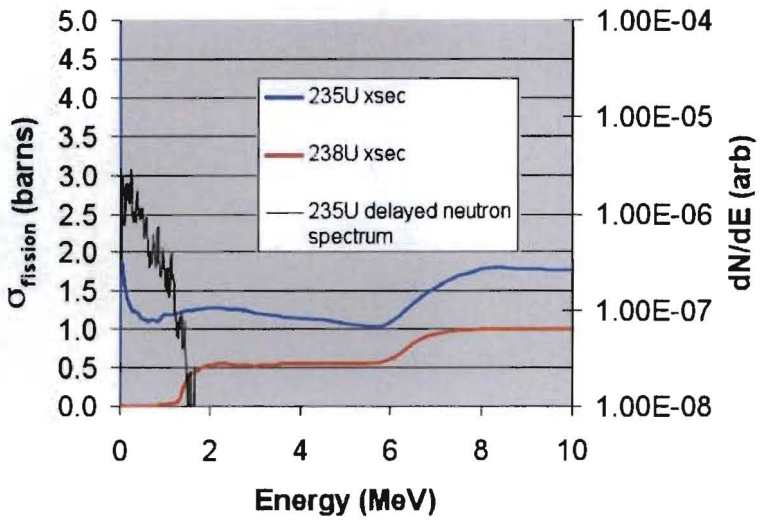

Figure 12. Comparison of the ^{235}U and ^{238}U fission cross sections as a function of the neutron energy.

---

[1] C. E. Moss, C. L. Hollas, G. W. McKinney, and W. L. Myers, "Comparison of Active Interrogation techniques," *IEEE Transactions on Nuclear Science*, **53** (2006) 2242.

[2] "Proton-Induced Fission Cross Section Calculation with the LANL Codes CEM2k+GEM2 and LAQGSM+GEM2," Mircea I. Baznat, Konstantin K. Gudima, Stepan G. Mashnik, arXiv:nucl-th/0307014 v1 2 Jul 2003.

[3] H. Ohm, W. Rudolph, K. L. Kratz, "Beta-delayed neutron emission following decay of ^{17}N," *Nucl. Phys. A.* **274** (1976) 45–52.

[4] K. S. Krane, *Introductory Nuclear Physics,* (John Wiley & Sons, New York 1988) pp. 304–306.

[5] I. Dostrovsky, R. Davis, Jr., A. M. Poskanzer, and P. L. Reeder, "Cross sections for the production of ^{9}Li, ^{16}C, and ^{17}N in irradiations with GeV-energy protons," *Phys. Rev.* **139**, (1965) B1513–B1524.

LA-UR-08-05741

Proton interrogation

Christopher L. Morris, for the PrI collaboration

Los Alamos National Laboratory, Los Alamos, NM 87544

Energetic proton beams may provide an attractive alternative when compared to electromagnetic and neutron beams for active interrogation of nuclear threats because: they have large fission cross sections, long mean free paths and high penetration, and proton beams can be manipulated with magnetic optics. We have measured time-dependent cross sections for delayed neutrons and gamma-rays using the 800 MeV proton beam from the Los Alamos Neutron Science Center for a set of bare and shielded targets. The results show significant signals from both unshielded and shielded nuclear materials. Results will be presented.

Why use protons for active interrogation*?

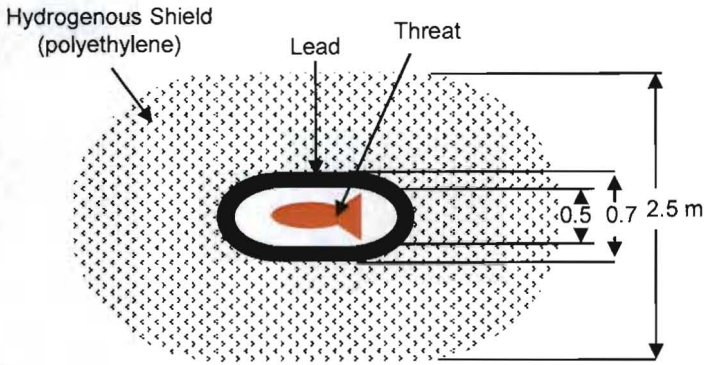

- Intermediate energy proton fission cross section is large.
- Proton mean free path is long.
- Proton transmission is large.
- Protons provide dose amplification in the target: 1 neutron/30MeV

*C. L. Morris, Fesseha Mariam and R. Schirato, *LANL*, John McGill, *GA*, *"Proton Interrogation", White paper presented to DNDO, 2005.*

LANSCE 800 MeV proton radiography facility

Confinement vessel

Camera Set 1

Camera Set 2

Delayed Neutron Measurement

- **Materials spanning the periodic tabe**
  - ^{12}C to ^{238}U
- **Simple targets**
  - 10s or 100s of gram samples
- **Simple counters**
  - ^{3}He gas mixture proportional counter
  - LaBr

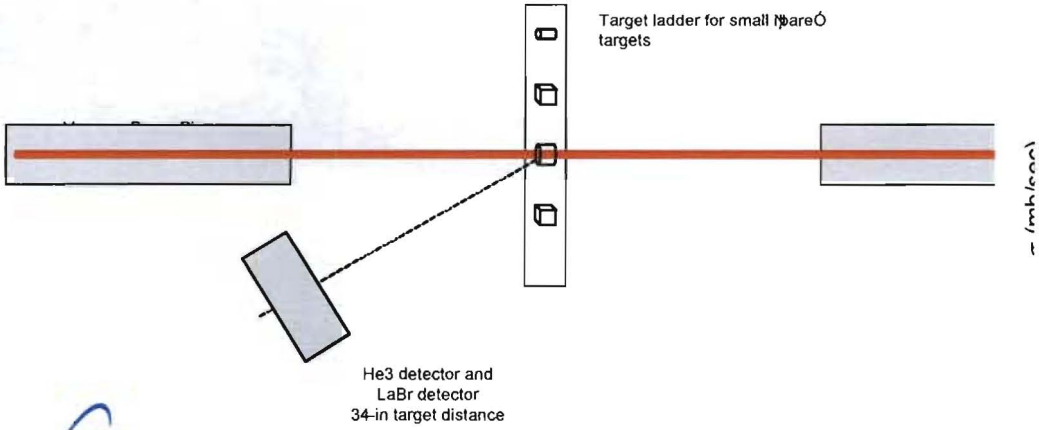

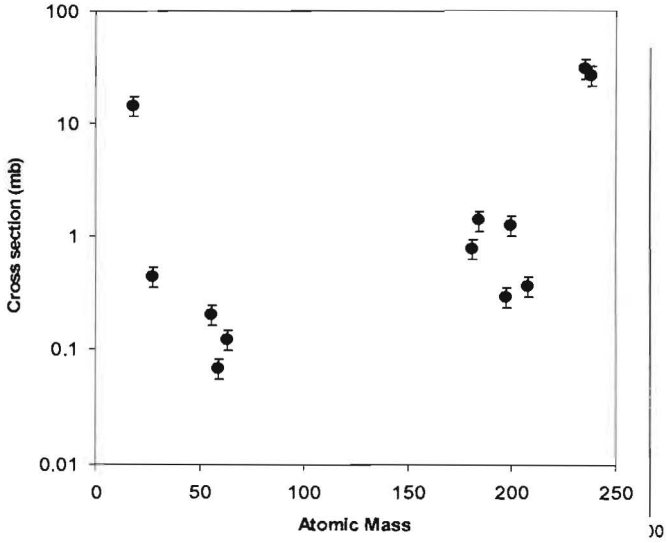

time, seconds

Delayed Neutron Measurement

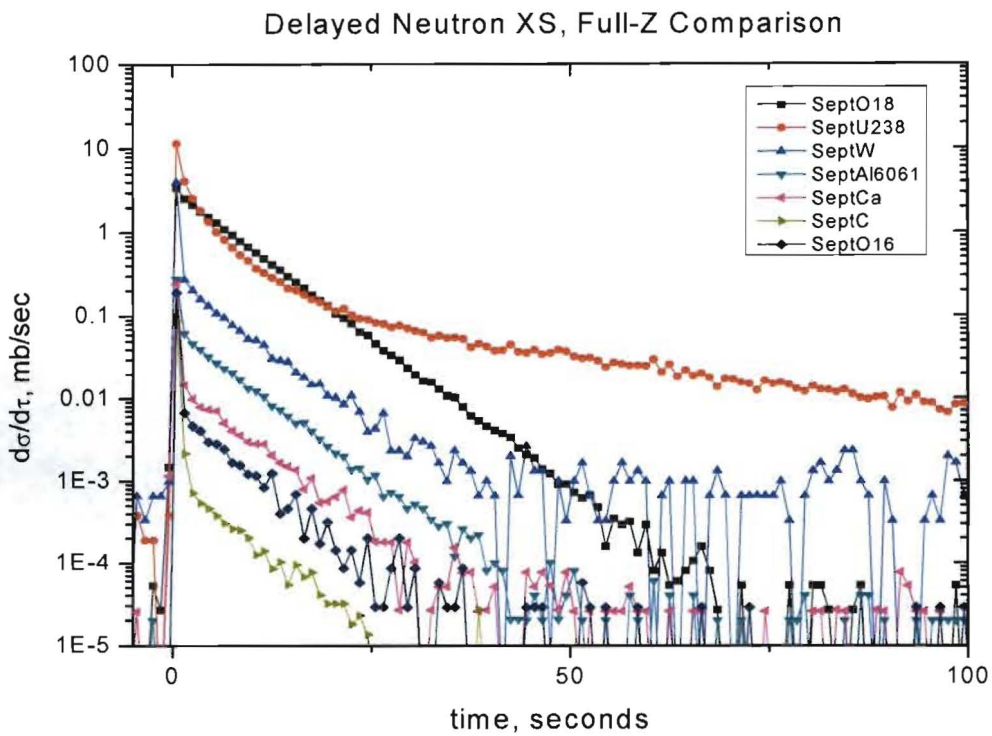

Delayed Gamma Ray Measurement

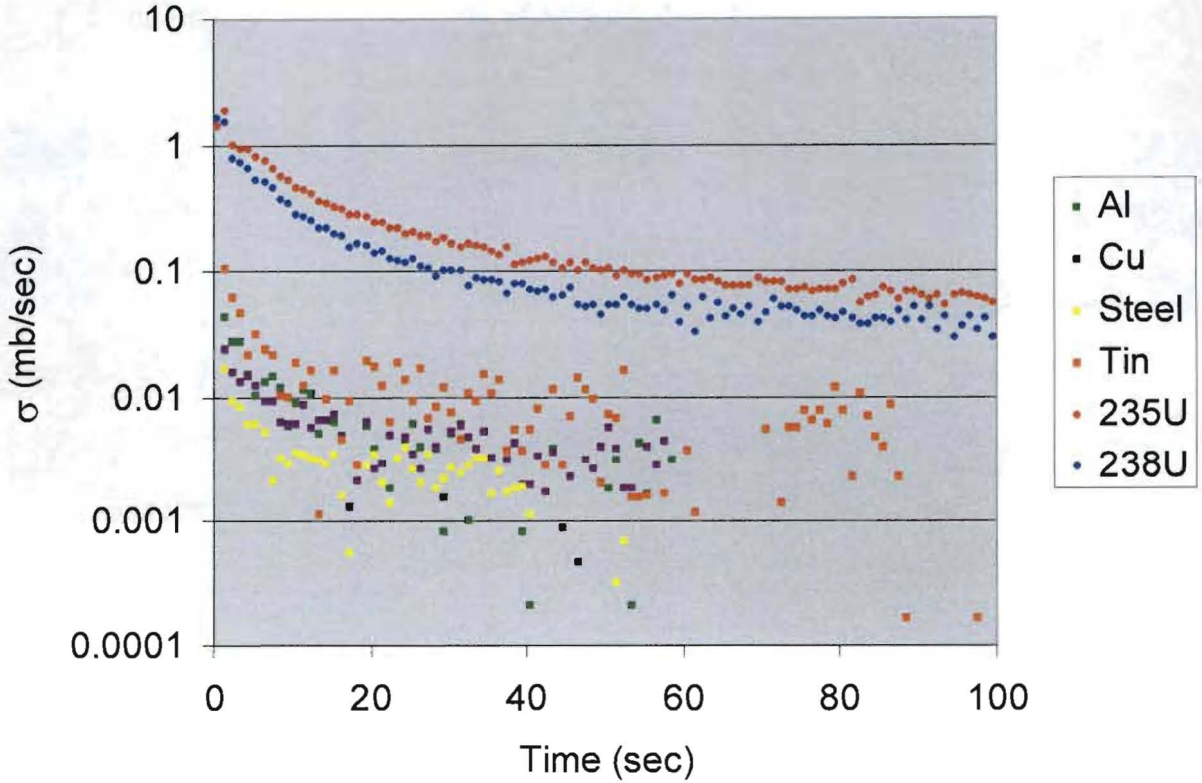

Delayed Neutrons

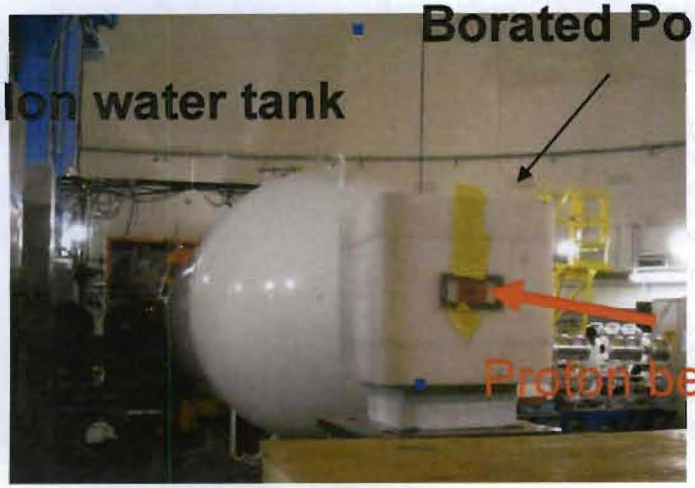

Neutron Detector @ 10 m

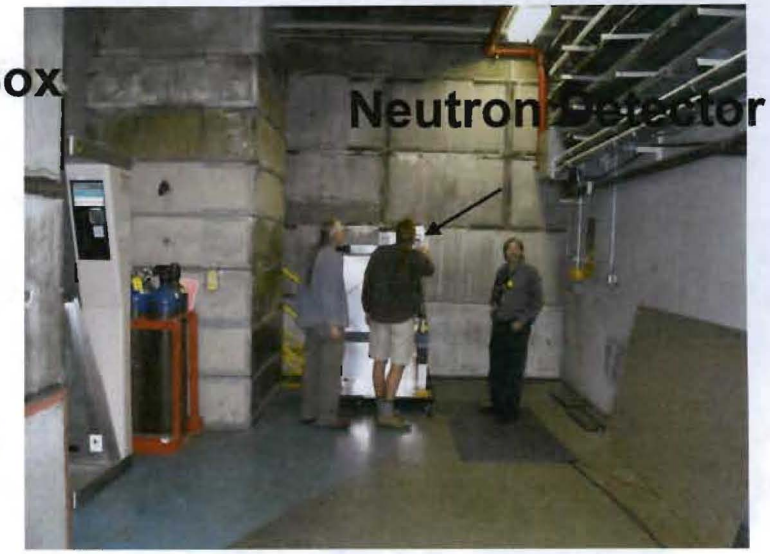

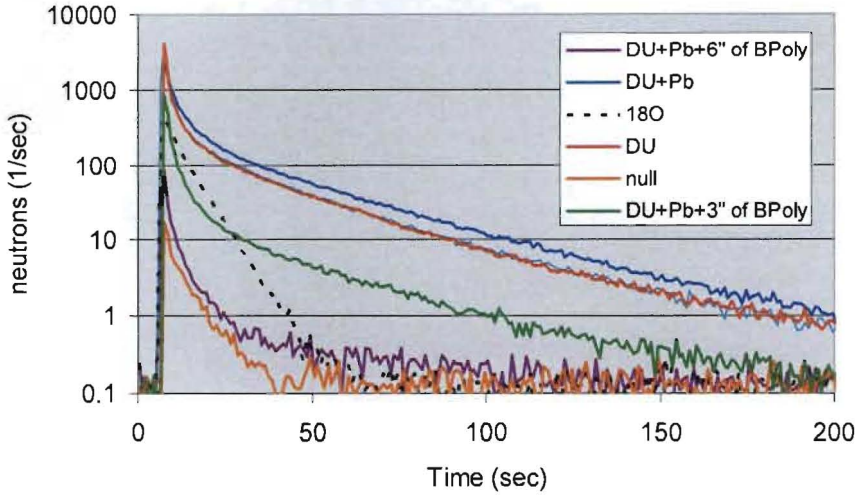

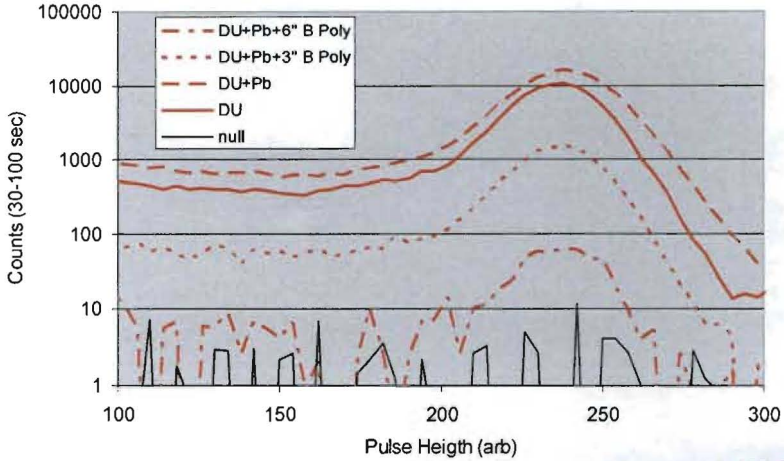

Delayed Neutrons

- Delayed neutrons(>4sec) signal fission
- Overburden increases signal
- Borated poly reduces signal

Signal to noise considerations

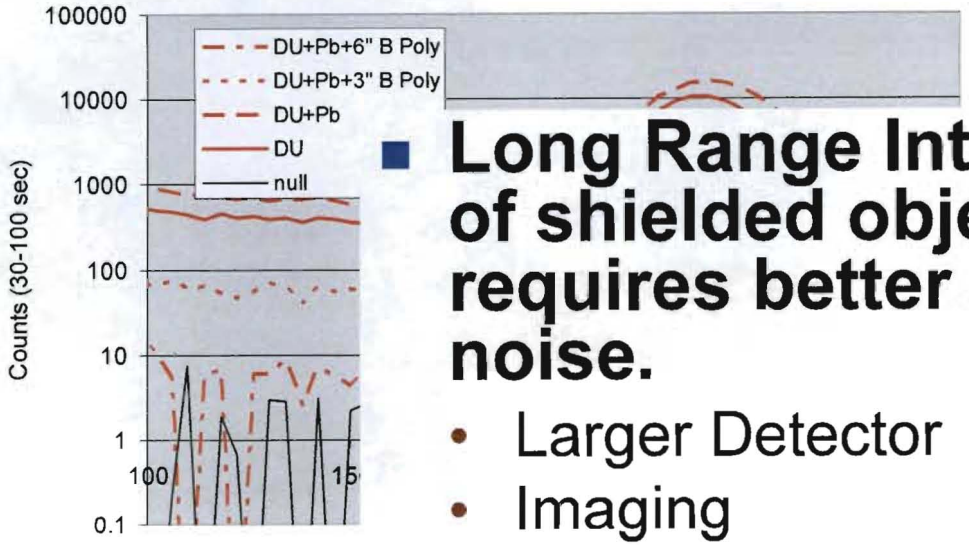

- **Long Range Interrogation of shielded objects requires better signal to noise.**
  - Larger Detector
  - Imaging
  - Energy Selection
  - Using other signals

If R_D is the distance to the detector and R_B is the radius at the object

$$\frac{{}_D{}^2 R_B{}^2)}{R_D{}^2}$$

$$/(R_D R_B{}^2)$$

	6" B Poly	3" B Poly	DU+Pb	DU
Counts	6.83E+02	1.36E+04	1.60E+05	9.52E+04
S/N 28.6 rad	72.45138	1439.835	17012.04	10101.03
S/N 0.1 rad	4.29E+00	8.52E+01	1.01E+03	5.98E+02

delayed rrac	0.005
delayed n	1.33E+09
fissions	2.66E+11

fissions/p

measured	2.33
model	1.6

Signal to noise considerations

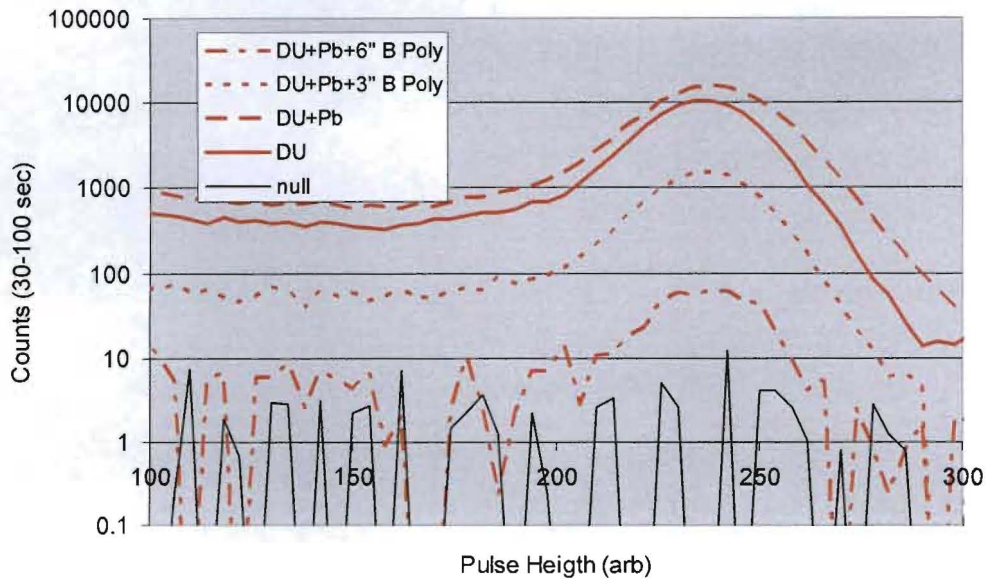

	6" B Poly	3" B Poly	DU+Pb	DU
Counts	6.83E+02	1.36E+04	1.60E+05	9.52E+04
S/N 28.6 rad	72.45138	1439.835	17012.04	10101.03
S/N 0.1 rad	4.29E+00	8.52E+01	1.01E+03	5.98E+02

If R_D is the distance to the detector and R_B is the radius of the beam at the object

$$S \propto 1/(R_D{}^2 R_B{}^2)$$

$$N \propto \sqrt{1/R_D{}^2}$$

$$S/N \propto 1/(R_D R_B{}^2)$$

$\Omega/4\pi$	8.77E-04
eff	0.3
delayed rrac	0.005
delayed n	1.33E+09
fissions	2.66E+11

fissions/p

measured	2.33
model	1.6

Signal to noise considerations

- **Long Range Interrogation of shielded objects requires better signal to noise.**
  - Larger Detector
  - Imaging
  - Energy Selection
  - Using other signals

Energy measurement

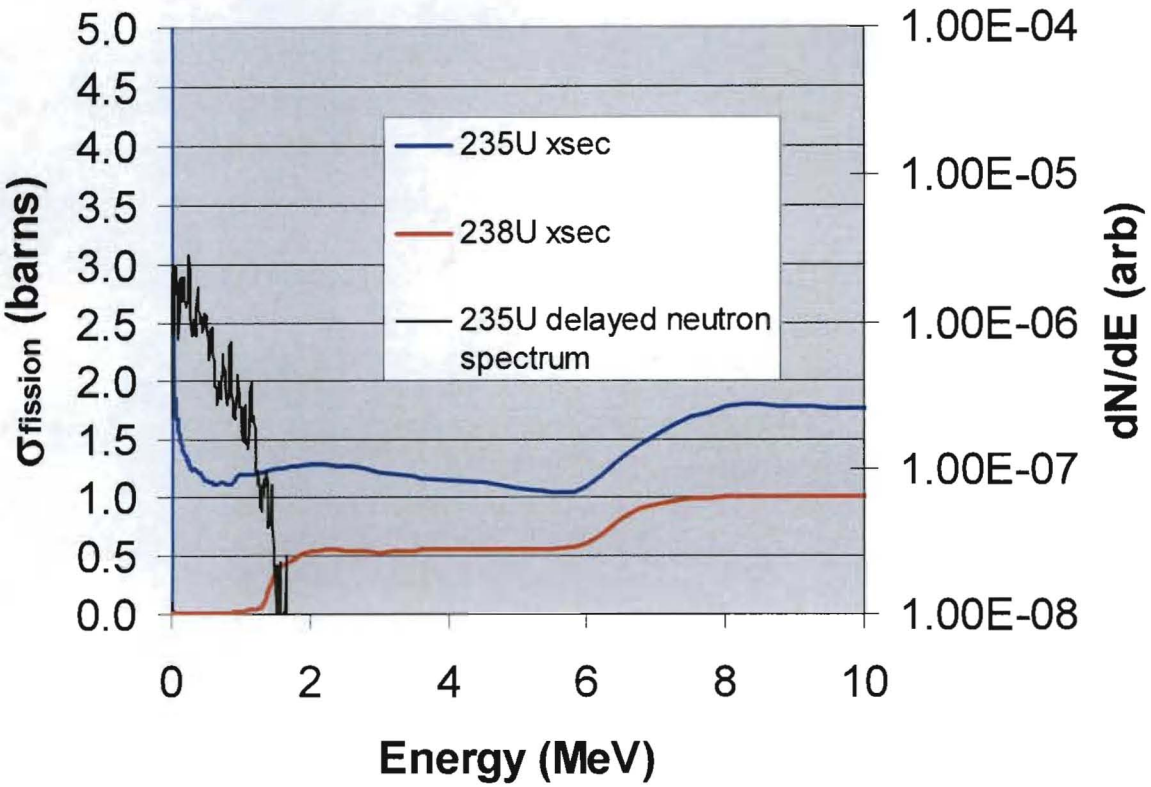

- β–delayed neutrons are all below 1 MeV.
- β–delayed Induce fission in ^{235}U and ^{239}Pu but not ^{238}U.
- Fission neutrons are nearly all above 1 MeV
- E_n>1 MeV discriminates $^{235,238}U$.
- E_n>1.8 MeV Removes ^{17}N background

Energy measurement

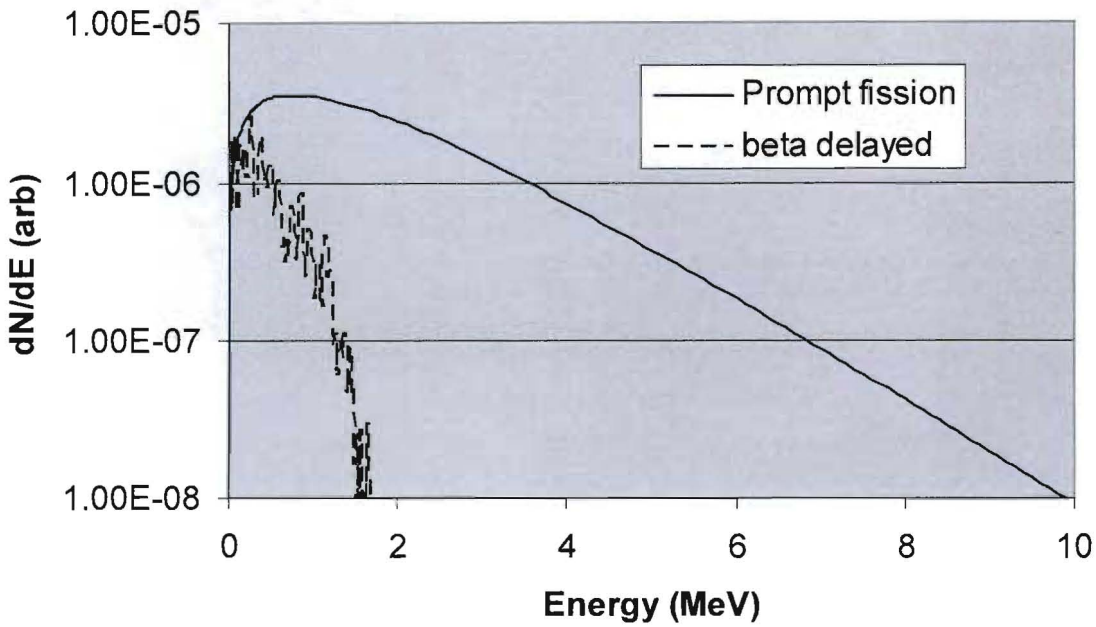

- β–delayed neutrons are all below 1 MeV.
- β–delayed Induce fission in ^{235}U and ^{239}Pu but not ^{238}U.
- Fission neutrons are nearly all above 1 MeV
- E_n>1 MeV discriminates $^{235,238}U$.
- E_n>1.8 MeV Removes ^{17}N background

Energy measurement

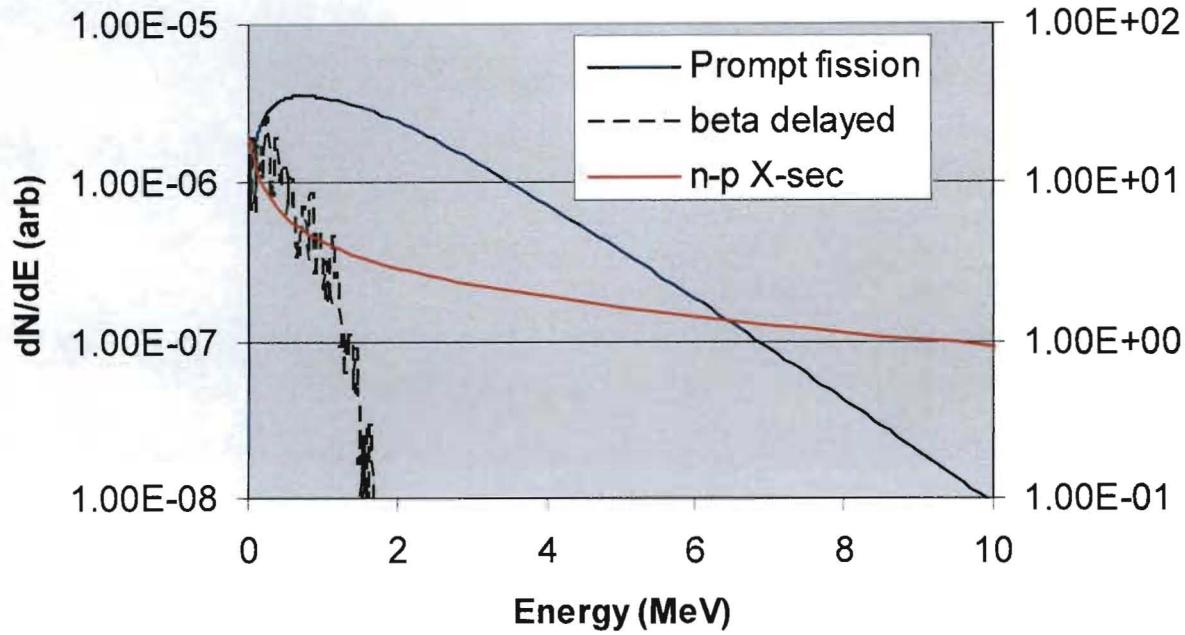

- β–delayed neutrons are all below 1 MeV.
- β–delayed Induce fission in ^{235}U and ^{239}Pu but not ^{238}U.
- Fission neutrons are nearly all above 1 MeV
- E_n>1 MeV discriminates $^{235,238}U$.
- E_n>1.8 MeV Removes ^{17}N background

Energy measurement

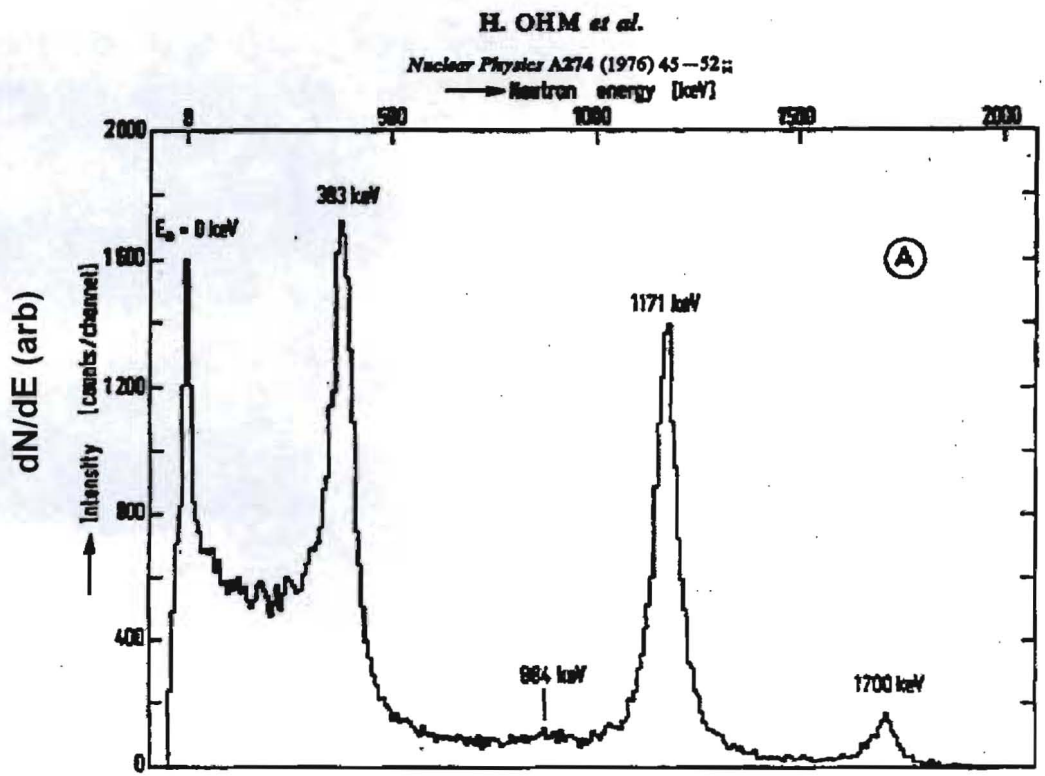

- β–delayed neutrons are all below 1 MeV.
- β–delayed Induce fission in ^{235}U and ^{239}Pu but not ^{238}U.
- Fission neutrons are nearly all above 1 MeV
- E_n>1 MeV discriminates $^{235,238}U$.
- E_n>1.8 MeV Removes ^{17}N background

5×10^8 protons/100 cm^2 (400 mrem) "remote" interrogation

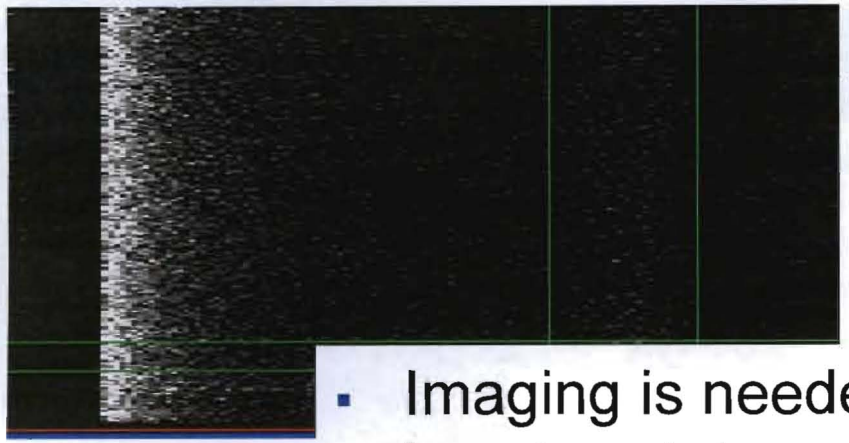

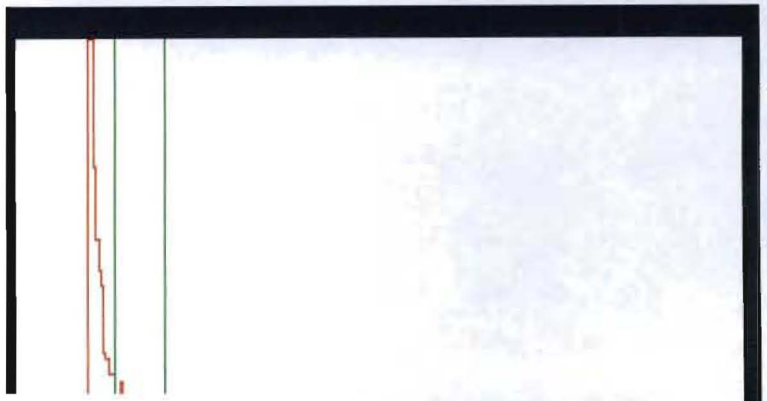

- Imaging is needed reduce the background for low dose interrogation.

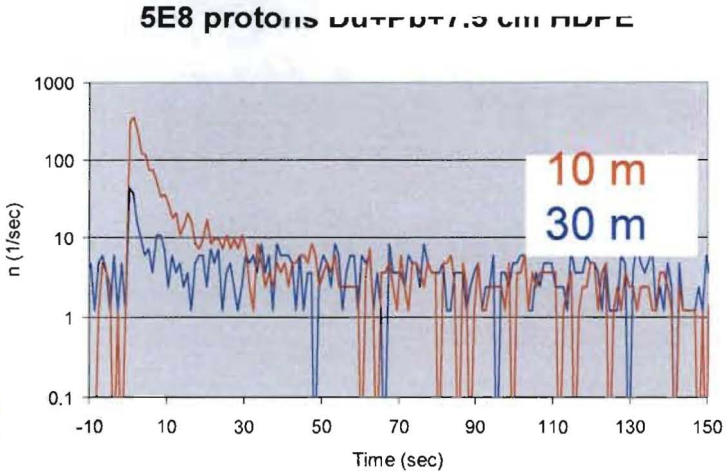

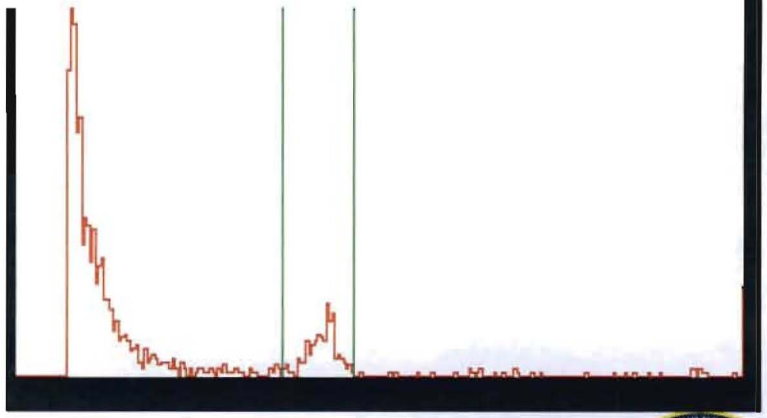

Detecting neutron shielding

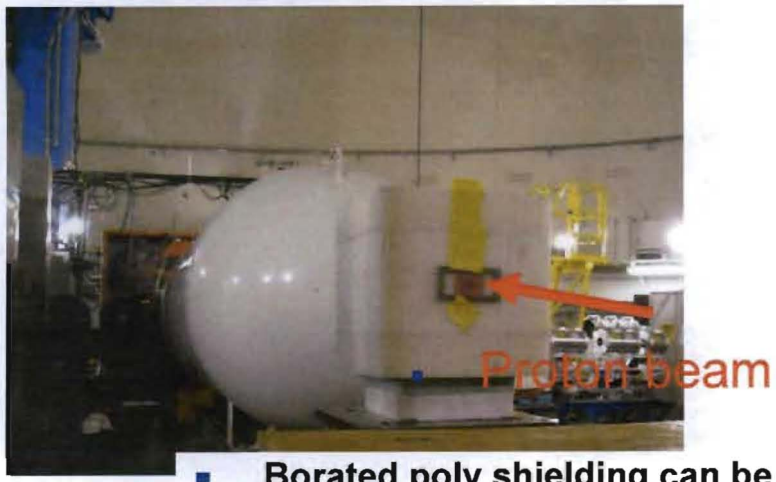

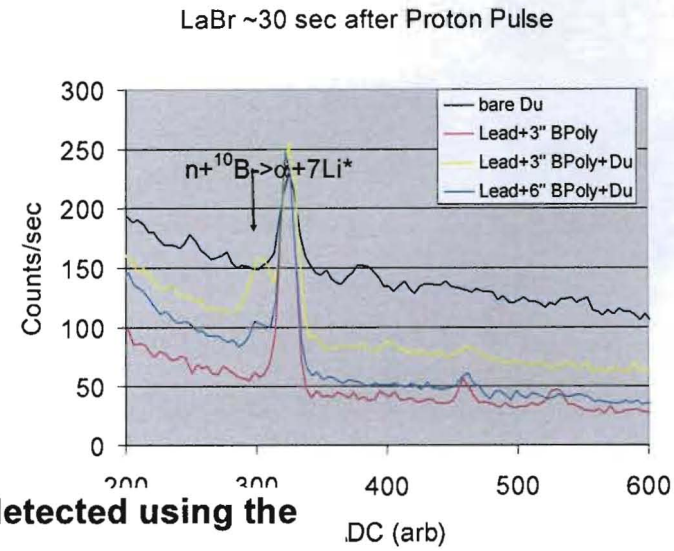

- **Borated poly shielding can be detected using the $^{7}Li^{*}$(480 keV γ)**

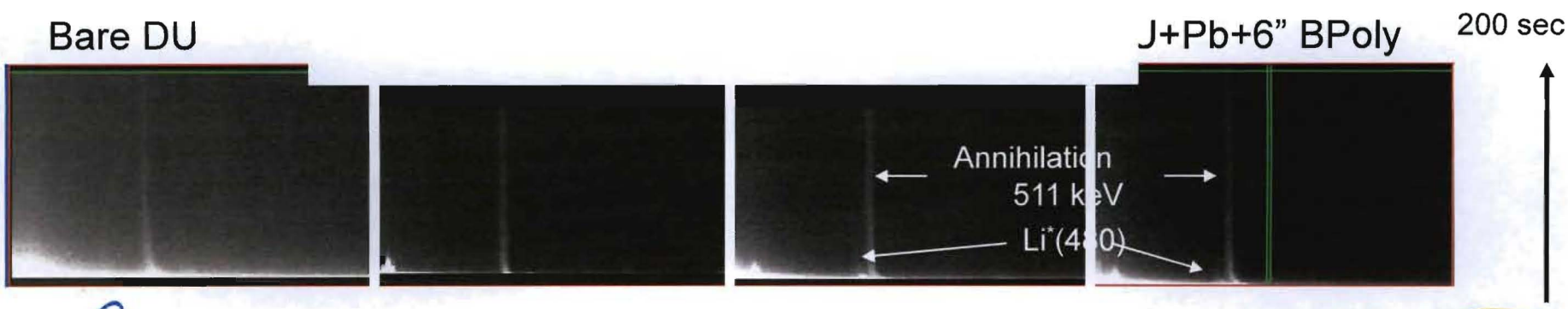

478 keV revisited with HPGe

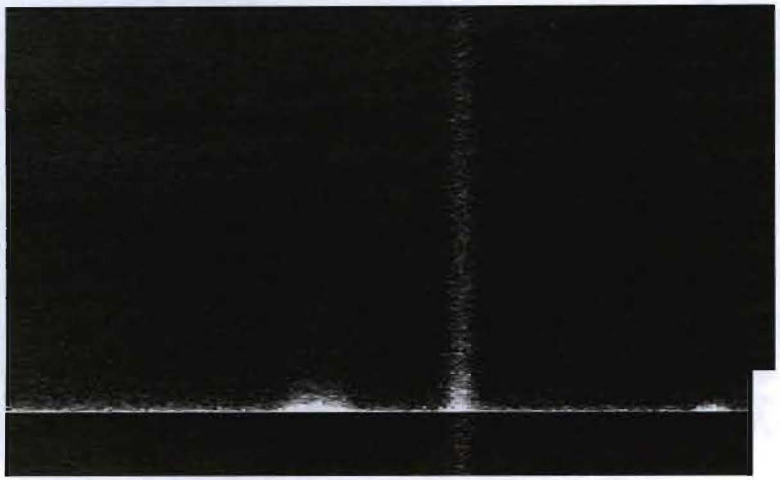

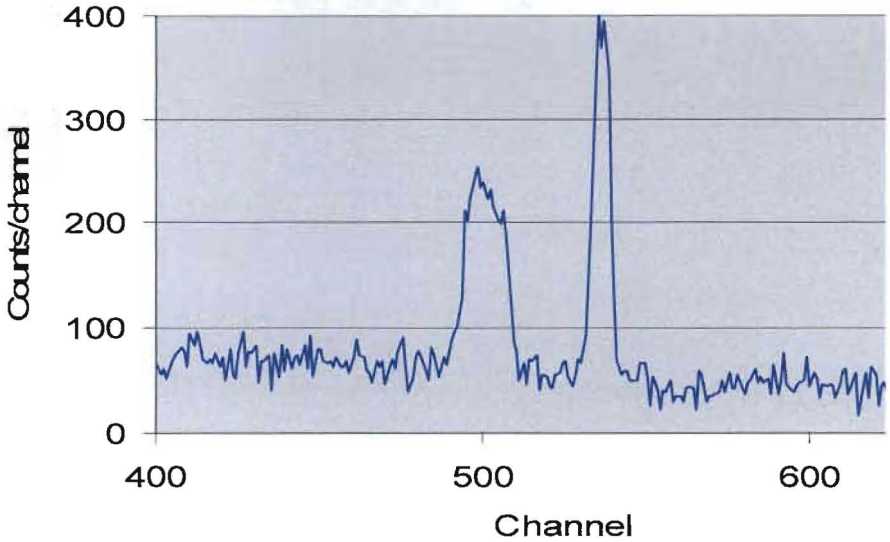

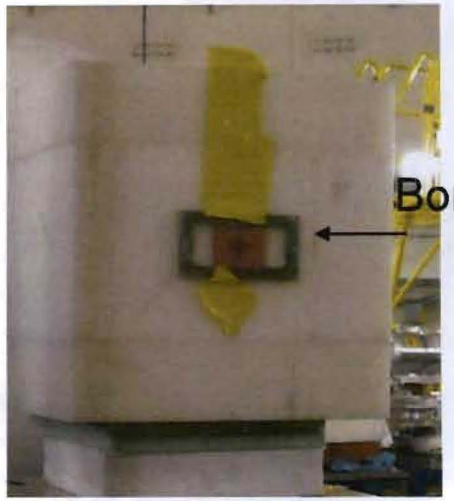

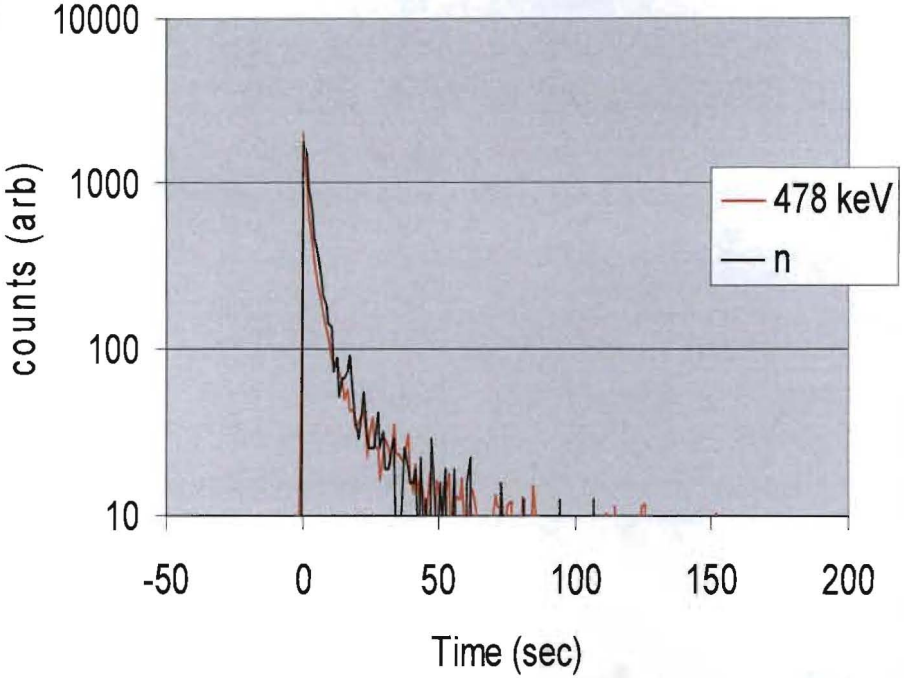

Delayed capture gamma rays-2200 keV n-p

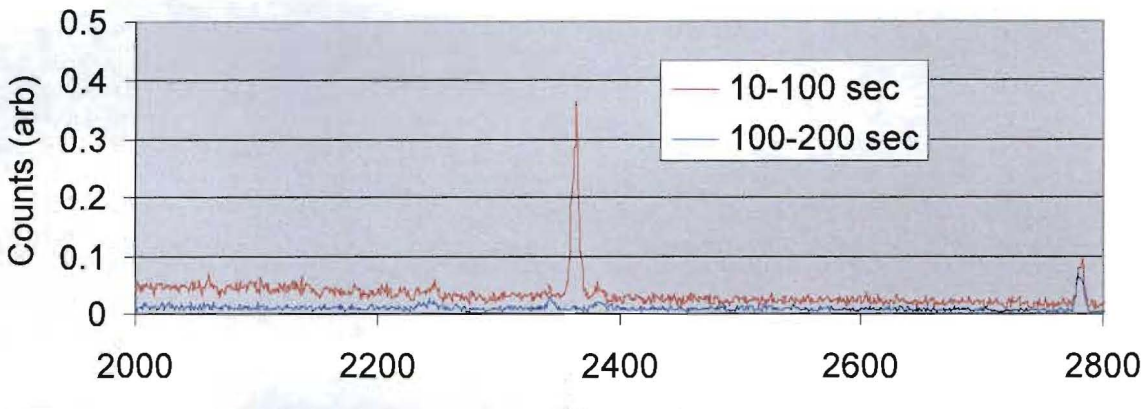

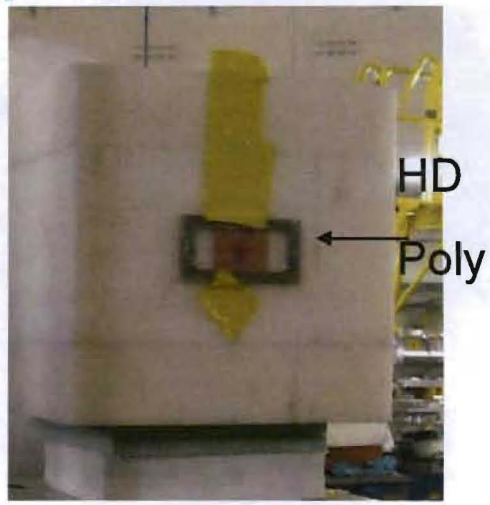

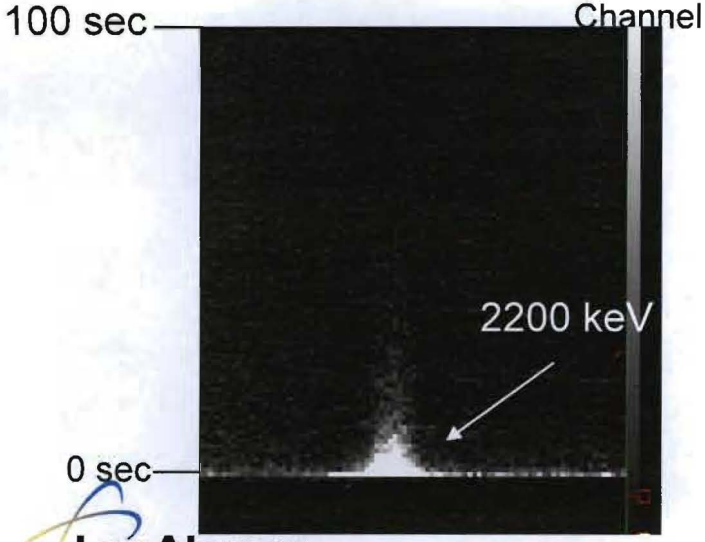

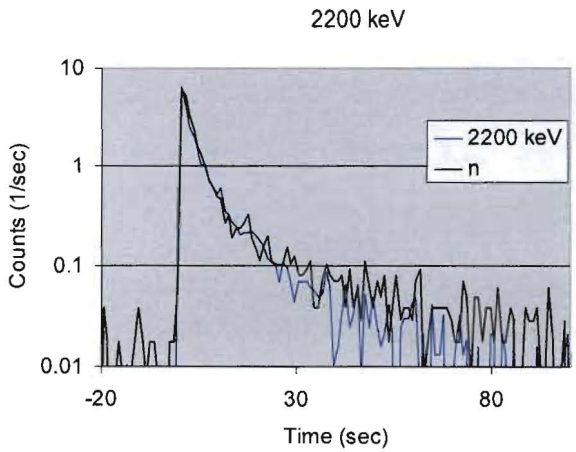

4Gev AGS Measurements

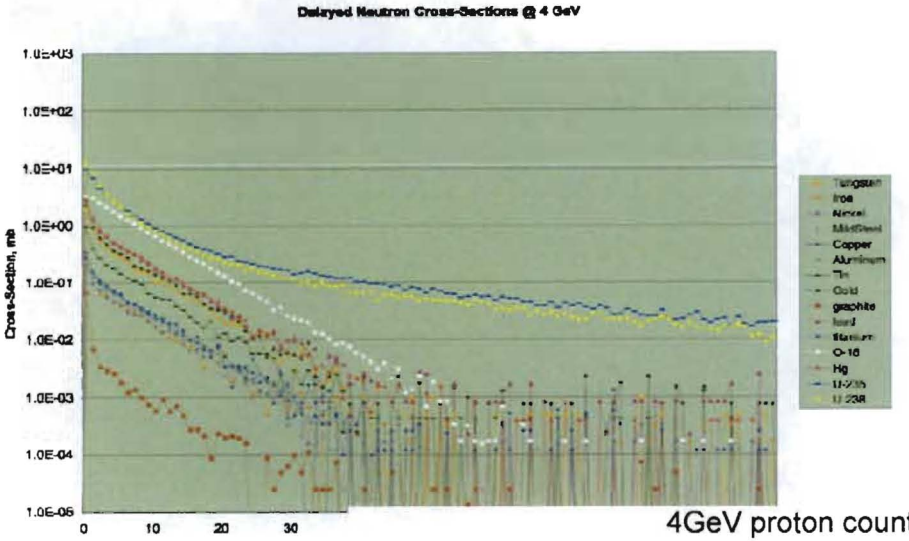

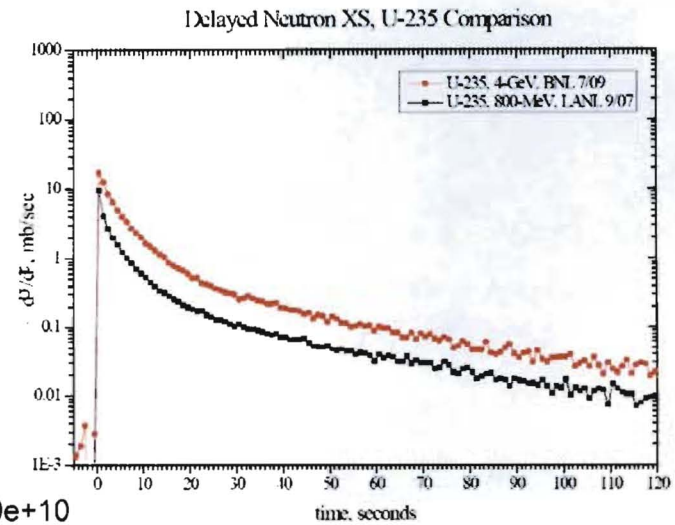

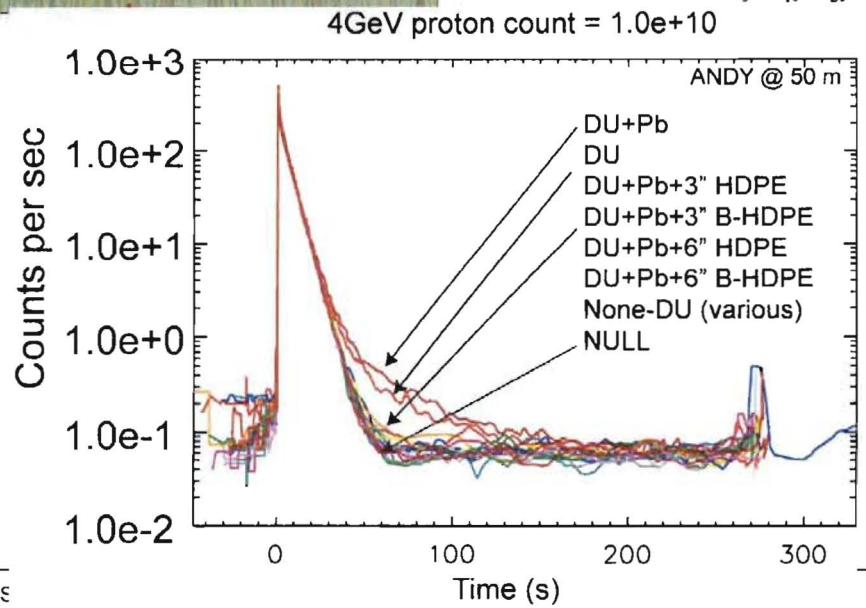

Accomplishments

- Measurements suggest proton induced delayed neutrons provide a significant signal of SNM at 800 MeV and 4 GeV
- Interrogation through significant overburden has been demonstrated
- Monte Carlo benchmarking under way